Phycologia (2006) Volume 45 (6), 616-623 Published 1 November 2006

Ultrastructure of the cyst wall of *Haematococcus pluvialis* (Chlorophyceae): wall development and behaviour during cyst germination

María Cecilia Damiani[1], Patricia I. Leonardi[1]*, Olga I. Pieroni[2] and Eduardo J. Cáceres[1]

[1]*Laboratorio de Ficología y Micología, Departamento de Biología, Bioquímica y Farmacia, Universidad Nacional del Sur, 8000 Bahía Blanca, Argentina*

[2]*Instituto de Química Orgánica, Departamento de Química, Universidad Nacional del Sur, Bahía Blanca, Argentina*

M.C. Damiani, P.I. Leonardi, O.I. Pieroni and E.J. Cáceres. 2006. Ultrastructure of the cyst wall of *Haematococcus pluvialis* (Chlorophyceae): wall development and behaviour during cyst germination. *Phycologia* 45: 616-623. DOI: 10.2216/05-27.1

The cell wall structure and behaviour of cysts of Argentinian strains of *Haematococcus pluvialis* were studied during cyst germination and zooid release. The cyst wall is composed of an outer primary wall, a trilaminar sheath, a secondary wall, and a tertiary wall. The primary wall disintegrates as the cyst ages. During germination the trilaminar sheath breaks down, carrying the adjacent secondary wall with it and the extensible tertiary wall accompanies the cyst in its size increase and shape changes. Zooid release subsequently follows as a result of the apical breakage of this third wall. Although the secondary and tertiary walls exhibit the same conformation in mature cysts, the arrangement of their components during their formation is different. This could be the reason why the behaviour of the two walls is different during germination. The chemical characterization carried out in the present research showed that the external trilaminar sheath of the wall is formed by algaenan, while fluorescence labelling suggested the presence of mannose and cellulose in the secondary and tertiary walls. Because of the physical difficulty of breaking cysts during astaxanthin extraction, cyst germination may provide a natural, alternative wall-breaking mechanism.

Key Words: Algaenan, Astaxanthin, Cell wall, Chlorophyceae, Cyst, Germination, *Haematococcus pluvialis*, Ultrastructure

INTRODUCTION

Haematococcus pluvialis Flotow is a freshwater unicellular, biflagellate microalga that may form cysts under extreme conditions. These cysts synthesize and store high amounts of astaxanthin, a secondary ketocarotenoid used as a natural colouring in aquaculture and the food industry (Johnson *et al.* 1980). Several studies on the culture parameters responsible for the formation of this pigment in *H. pluvialis* have been carried out in nonmotile cells (Harker *et al.* 1996) and motile cells (Hagen *et al.* 2000, 2001; Wang *et al.* 2003). The functional aspects of astaxanthin have also been investigated (Hagen *et al.* 1994).

Because of its high resistance to chemical, enzymatic, and mechanical attacks, the cyst wall of *H. pluvialis* constitutes a serious problem for astaxanthin-extraction procedures. To date, mechanical and autoclave treatments are the most effective methods of astaxanthin extraction and bioavailability (Mendes-Pinto *et al.* 2001).

The fine structure as well as the chemical composition of the cell wall of *H. pluvialis* has already been studied. Montsant *et al.* (2001) observed the presence of a nonhydrolyzable biopolymer in the wall of vegetative cells and cysts in populations found in Denmark. Hagen *et al.* (2002) reported changes in the fine structure and chemistry of the cell wall during the transformation of the flagellate cells into cysts in German *H. pluvialis* strains. They also claimed that motile biflagellate stages exhibit a gelatinous extracellular matrix and that the transformation into the nonmotile cell stage is characterized by the formation of a new layer, a primary wall, within the extracellular matrix. They also observed that a trilaminar sheath is formed inside the primary wall and that the innermost layer is an amorphous secondary wall.

The aim of the present research was to analyse the cell wall structure and behaviour in Argentinian strains of *H. pluvialis* during the germination of cysts and to chemically characterize the cyst wall. This is the first ultrastructural analysis conducted to date on the germination process in *H. pluvialis* cysts. In view of the physical difficulty of breaking cysts during astaxanthin extraction (Mendes-Pinto *et al.* 2001), a detailed knowledge of the cell wall structure as well as the behaviour and chemistry of its different layers is important for designing an alternative, natural wall-breaking mechanism.

MATERIAL AND METHODS

Sampling

H. pluvialis samples were obtained from rainwater in Bahía Blanca, Buenos Aires Province, Argentina. They were collected in 40 cm deep inverted fiberglass pyramidal receptacles. Unialgal cultures were obtained by means of serial dilutions (Stein 1973).

Culture conditions

Motile cells were cultured in a Bold's Basal Medium (BBM) at 20–22°C and under a 12 : 12 h light : dark regime by illumination with cool-white fluorescent lamps providing 67 μmol photons m^{-2} s^{-1} at pH 7–7.5. Maintaining the vegetative

* Corresponding author (leonardi@uns.edu.ar).

cells without medium renewal during a period longer than 20 days induced cyst formation. Sporocyst germination was achieved by desiccation in a stove at 40°C and subsequent transfer to a fresh medium for 4 days. Gametocyst germination was induced by transferring the cysts to distilled water for 3 days before a subsequent transfer to a fresh medium.

Transmission electron microscopy

Cysts were fixed at 5°C either in (1) 3% glutaraldehyde and 1.5% paraformaldehyde in 0.05 M sodium cacodylate buffer (pH 7.4), or (2) in 3% glutaraldehyde and 1.5% acroleine in 0.05 M sodium cacodylate. In both cases, the fixation period lasted 1 wk, and was achieved by keeping the cysts for 12 h under reduced pressure in a desiccator. After four washes in sodium cacodylate buffer, the samples were postfixed in 2% OsO_4 in sodium cacodylate buffer, washed in sodium cacodylate buffer, dehydrated in an acetone series, and infiltrated with Spurr's low-viscosity resin with continuous agitation during a week. They were subsequently embedded in resin following the flat method (Reymond & Pickett-Heaps 1983). The sections were cut with a diamond knife, stained with uranyl acetate and lead citrate, and viewed with a Jeol 100 CX-II electron microscope. The aceto-resistant materials were fixed for transmission electron microscopy (TEM) as indicated above.

Scanning electron microscopy

Cells were fixed in 2% glutaraldehyde in a sodium cacodylate 0.05 M buffer at 5°C, and they were left to settle on glass coverslips coated with 5% poly-D-Lysine (Sigma). They were subsequently postfixed in 0.01% OsO_4, dehydrated in an acetone series, and dried in a critical-point dryer. Coverslips were fastened to bronze stubs, coated with gold in a sputter coater, and samples were viewed in a JEOL SM-35 CF scanning electron microscope.

Chemical analysis of cell wall components

Mature cysts of *H. pluvialis* were tested for sporopollenin-like components via acetolysis. Cells were first concentrated by centrifugation for 3 min. They were then resuspended in 2–3 ml of a freshly prepared solution of acetic anhydride : sulfuric acid (9 : 1 v/v). The centrifuge tubes were immersed in a boiling water bath for 15–20 min. The acetolysis mixture was subsequently diluted by the addition of 40 ml of distilled water and centrifuged for 10 min. The pellet was finally resuspended and washed with four changes of distilled water. In addition, the cysts were treated with (1) chromic acid at room temperature for 5 h (Puel *et al.* 1987), (2) 10% KOH at 100°C for 45 min (Delwiche *et al.* 1989), (3) 2-aminoethanol at 95°C for 1 h (Southworth 1974), and (4) 2% phloroglucinol in 95% ethanol for several minutes followed by the drop-wise addition of HCl 50% (phloroglucinol test for lignin; Puel *et al.* 1987).

Spectroscopic analysis of the aceto-resistant material

Infrared spectrum was obtained by means of Diffuse Reflectance Infrared Fourier Transform Spectroscopy (DRIFTS) using the microsampling cup of an Avatar diffuse reflectance accessory (1.50 mg of dried material in 150 mg of dried KBr) against a KBr background on a Nicolet-Nexus 470 FT-IR spectrometer (DTGS detector Nichrome source; Beamsplitter: KBr) with a total of 64 scans.

Enzymatic treatment of the cyst cell walls

Cell walls of mature cysts were broken by repeated tip ultrasonication (at a maximum frequency of 20 Hz) in an ice bath in order to allow enzymatic digestion with the following two enzymes: cellulase EC 3.2.14 (Sigma, C-8546), 5.8 units enzymatics (u.e.) in 0.5 ml of 0.05 M citrate buffer pH 4.8, and β-mannosidase EC 3.2.25 (Sigma, M-9400), 0.046 u.e. in 0.5 ml of 0.05 M citrate buffer pH 4.8. In both cases, incubation was carried out with constant stirring at 45°C for 2 days. Enzymatically digested cyst residues were repeatedly washed with water by centrifugation, then stained with an aqueous solution of 0.01% Calcofluor White for 30 s. The material was again washed with water and observed in a Zeiss Axiolab microscope equipped with epifluorescence.

RESULTS

Cyst formation

The flagellate cells (Fig. 1) that were kept under stress conditions during 3 wk, at which point their protoplasts became rounded, increased in size and lost motility (Figs 2, 3), forming cysts (Figs 4, 5). At cyst maturity the vegetative wall disappeared (Fig. 5). The diameter of cysts ranged between 22 μm and 76 μm. Electron microscopy revealed that the cyst wall was composed of an outer primary wall, a trilaminar sheath, and a secondary wall, in agreement with the observations by Hagen *et al.* (2002) in German strains. However, in the present study an additional tertiary wall was observed. The primary wall disintegrated gradually as the cyst aged (Figs 6–8). Scanning electron microscopy (SEM) observations revealed that the surface of the trilaminar sheath was irregularly wavy (Fig. 9).

In 4- to 6-week-old cysts a fibrous tertiary wall consisting of two layers could be observed. An electron dense material came into contact with the internal surface of the secondary wall (Fig. 10). This first stratum exhibited a lax spongy texture (Fig. 11). The second stratum was formed later by the deposition of material in a more compact fashion (Fig. 11). Throughout synthesis the tertiary wall maintained the same bilayered configuration (Fig. 12, TW1 and TW2). After 6 wk, these strata finally compacted themselves and the tertiary wall reached the same homogeneous appearance as that of the secondary wall. Both walls could be clearly distinguished by the presence of a thin electron translucent layer between them (Fig. 13).

Cyst germination

The cell wall behaviour during germination was identical in sporocysts and gametocysts. After the transfer to a fresh medium, cysts germinated and gave rise either to 8–16 zoospores (Fig. 14) or 16–32 isogametes (Fig. 15), respectively, in accordance with the culture conditions described in the Material and Methods section. During cyst germination and zooid release, the cyst wall components behaved differently. Whereas

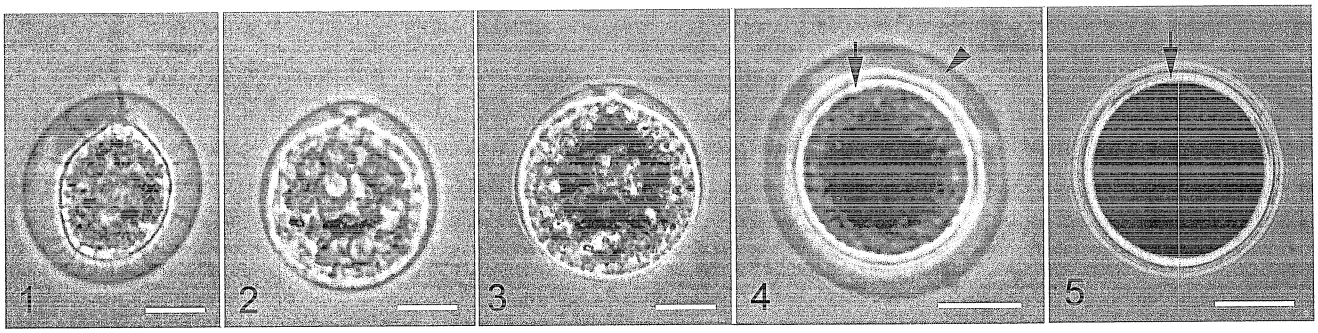

Figs 1–5. Formation of cysts in *H. pluvialis* (light micrographs).
Fig. 1. Vegetative cells growing in Bold's Basal Medium.
Figs 2, 3. Vegetative cells under 10- and 15-day stress conditions, respectively. Note that the protoplast has not only rounded but has also increased in size.
Fig. 4. Not fully mature cyst under 3-wk stress conditions. Note the cyst wall (arrow) inside the vegetative wall (arrowhead). Astaxanthin is present only in the middle of the cell.
Fig. 5. Fully mature cyst plenty of astaxanthin under 6-wk stress conditions. Note the absence of the vegetative cell wall. The arrow indicates the cyst wall. Scale bars = 10 μm.

the trilaminar sheath broke down, carrying the adjacent secondary wall (Figs 16, 17), the extensible tertiary wall accompanied the cyst in its size increase and shape changes (Figs 16, 17). In addition, the tertiary wall exhibited the same ultrastructural configuration as that observed during its synthesis in 4- to 6-wk-old cysts (compare Fig. 12 and Fig. 18). Zooids were then released upon breakage of this third wall, which became very thin in the apical area (Fig. 19). At this stage, zooids conserved the cysts' reddish colouring due to astaxanthin. Empty cysts maintained the same shape as the one they had during their germination (Fig. 20).

Chemical characterization of the cyst wall

In the present research it was observed that the cyst wall in *H. pluvialis* was extremely resistant to nonoxidative treatments such as acetolysis. In relatively small cysts the acetolysed walls maintained their spherical shape (Fig. 21) while they collapsed – appearing crumpled – in larger cysts. TEM observations revealed that the aceto-resistant materials had their typical trilaminar appearance [i.e. an electron translucent stratum located between two electron dense strata (Fig. 22)].

The cysts treated with 10% KOH and 2-aminoethanol exhibited no alterations in their walls (Figs 23 and 24, respectively). Mature cysts were incubated in chromic acid at room temperature and their wall dissolved after 5 h (nonillustrated observations). The dyeing reactions for lignin were negative in the cyst wall.

Mature cysts stained with Calcofluor White and irradiated with UV light exhibited a continuous fluorescence in their walls (Fig. 25). After treating these cysts with cellulase, fluorescence decreased in both the trilaminar sheath and the secondary wall while the tertiary wall showed discontinuous fluorescence (Fig. 26). The treatment of cysts with β-mannosidase did not affect fluorescence in the trilaminar sheath, although it decreased in the secondary wall and was discontinuous in the tertiary wall (Fig. 27).

The infrared spectroscopic analysis of aceto-resistant materials revealed three regions shown in the FT-IR spectrometer (Fig. 28). The first one, ranging between 4000 and 1800 cm^{-1}, exhibits a broad band centered at about 3380 cm^{-1} (**1**), which corresponds to the absorption caused by the stretching of −OH bands. The two sharper peaks, which are respectively located between 2920 (**2**) and 2850 cm^{-1} (**3**), result from out-of-phase CH_2 and in-phase CH_3 stretching. The second region ranging between 1800 and 1500 cm^{-1} is the area of carbonyl and the C=C double bond. Its first peak, which is located at about 1740 cm^{-1} (**4**), could be attributed to the carbonyl stretching vibration of esters and ketones (Pappas *et al.* 1999). The second peak, which is located at about 1530 cm^{-1} (**5**), reveals the absorption of both C=C double bonds and the carboxylate group (Sene *et al.* 1994). The third region, which is located between 1500 and 800 cm^{-1}, is associated with the skeletal vibrations of the components. Five absorption bands were observed. The first one, which is located at 1470 cm^{-1} (**6**), could be attributed to asymmetric $-CH_2$ and $-CH_3$ in-plane bending vibrations (Pretsch *et al.* 1983). The second band, which is located at 1370 cm^{-1} (**7**), correlates with −OH

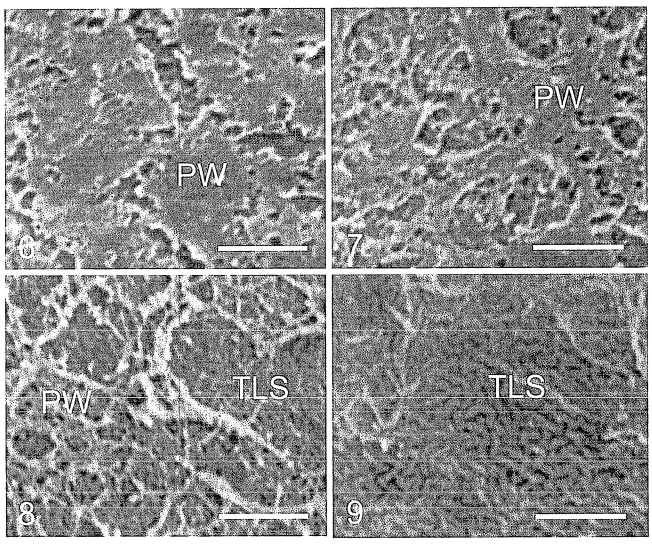

Figs 6–9. SEM micrographs of 4/5-wk-old cysts.
Figs 6–8. Details of the successive gradual breakage and disintegration of the primary wall. Scale bars = 1 μm.
Fig. 9. The primary wall has completely disappeared, clearly revealing the irregularly wavy surface of the trilaminar sheath. PW, primary wall; TLS, trilaminar sheath. Scale bar = 1 μm.

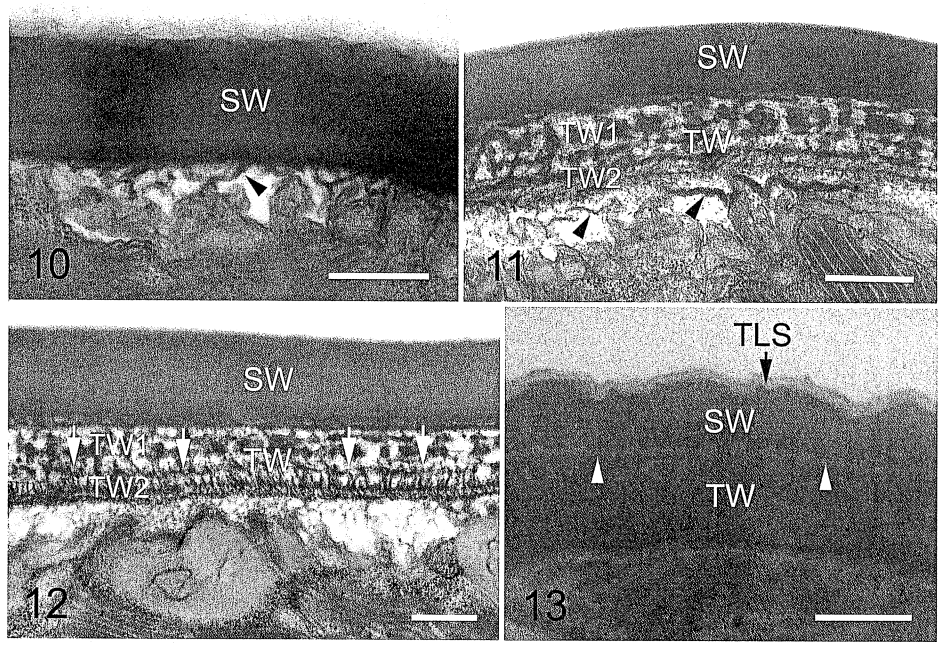

Figs 10–13. Development of the tertiary wall in 4/6-wk-old cysts of *H. pluvialis* (TEM micrographs).
Fig. 10. Initial synthesis of the first stratum by deposition of electron-dense material adjacent to the secondary wall (arrowhead).
Fig. 11. A lax spongy stratum (TW1) is in contact with the secondary wall, whereas a second stratum (TW2) is in the process of formation due to the deposition of material (arrowheads) in a more compact fashion.
Fig. 12. The tertiary wall is almost fully synthesized although it conserves the same bilayered configuration as the one it displays during the formation process (TW1 and TW2). The arrowheads indicate the boundary between both strata.
Fig. 13. The tertiary wall is completely formed, its final appearance looks homogeneous and compact. The arrowheads show the thin electron translucent layer between the secondary and tertiary walls. Scale bars = 0.5 μm. SW, secondary wall; TLS, trilaminar sheath; TW, tertiary wall; TW1, first stratum of tertiary wall; TW2, second stratum of tertiary wall.

(bending vibration), C-O-H (in-plane bending vibration), $-COO^-$ (bending vibration), $-CH_3$ (in-plane bending vibration), and $-CH_2$ (wagging and twisting vibrations) (Nakanishi and Solomon 1977). The third band, which is located at 1235 cm^{-1} **(8)**, corresponds to $-OH$ (in-plane bending vibration) (Kokot *et al.* 1997). C-O from the ester carboxyl (stretching vibration) also absorbs in the same band **(8)**. The fourth band, which is located at 1160 cm^{-1} **(9)** −1045 cm^{-1} **(10)**, reveals the skeletal vibration of C-OH and C-O-C (Faust 1992). The fifth band, which is located at 910 cm^{-1} **(11)**, is typical of the out-of-plane bending vibration of C-H in *trans* carbon–carbon double bonds (Burczyk 1987).

DISCUSSION

Cyst formation

Mature cyst walls in Argentinian *H. pluvialis* populations clearly show the presence of an external trilaminar sheath and two walls; namely, a secondary one located in the middle, and an internal tertiary one. Both are fibrous, homogeneous, and compact. In their study on mature cysts of *Polytomella agilis* with freeze-etching techniques, Brown *et al.* (1976) also observed an additional, internal wall, which was similar to the neighbouring wall, in a configuration similar to that of the secondary and tertiary walls of our materials. Of interest, no third wall stratum was described by Hagen *et al.* (2002) in 4-wk-old to 3-mo-old cysts in German *H. pluvialis* strains analysed with freeze-etching and freeze-fracture techniques. Because the culture medium used in the study by Hagen *et al.* (2001) was different from that used in the present research, the absence of a tertiary wall in the cysts of the German strains could be due to a delay in its formation. It could be hypothesized that the German *H. pluvialis* strains analysed by Hagen *et al.* (2002) were not yet mature.

SEM observations revealed that the wavy surface of the trilaminar sheath in the Argentinian *H. pluvialis* cysts exhibited similarities with the exine ornamentation in the wall of pollen granules of some Crassulaceae and Ulmaceae (Iversen & Troels-Smith 1950; Hoen 2000). A similar surface morphology was also observed in the wall mesospore of *Spirogyra salmonispora* zygospores (Ferrer & Cáceres 1995).

Cyst germination

During germination, changes in the cyst shape – similar to those described for our materials – were observed in temporary cysts of the dinoflagellate *Alexandrium ostenfeldii* (Ostergaard Jensen & Moestrup 1997). The behaviour of the inner layers of their walls, which were observed with a light microscope, also resembles that of the tertiary wall of *H. pluvialis* cysts.

The particular behaviour of the components of *H. pluvialis* cyst wall during germination and zooid release is novel for green algae. In the present research it was observed that the trilaminar sheath and the secondary wall acted as if they were a single structure: both broke as a consequence of the increase in the cyst's size resulting during zooid formation. In contrast, the more flexible tertiary wall stretched out and accompanied

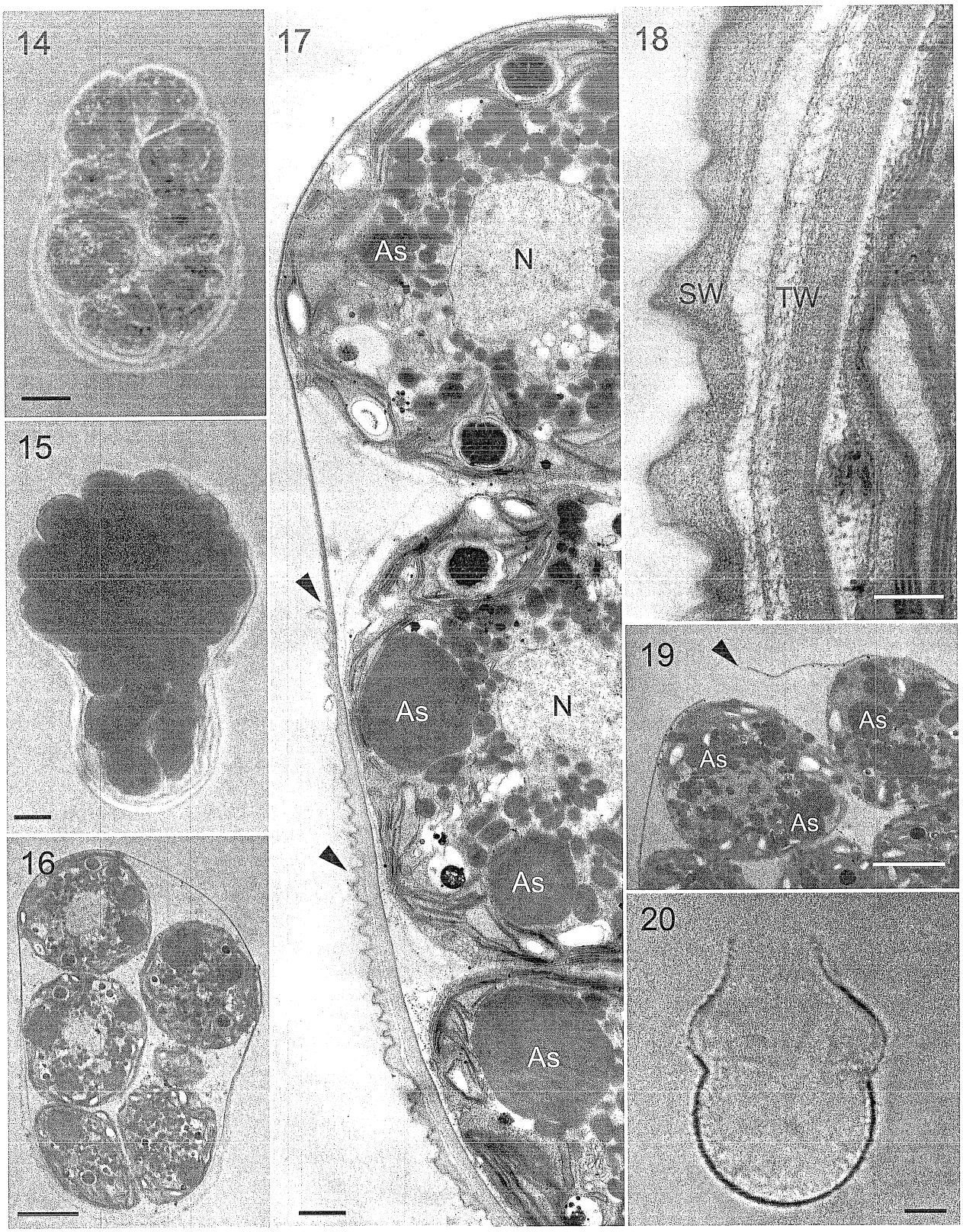

Figs 14–20. Cyst germination in *H. pluvialis.*
Fig. 14. Sporocyst (light micrograph).
Fig. 15. Gametocyst (light micrograph). Scale bars = 5 μm.
Figs 16–19. TEM micrographs.
Fig. 16. General view of the longitudinal section of a sporocyst. Scale bar = 5 μm.
Fig. 17. Further details of Fig. 16 showing the trilaminar sheath and its adjacent secondary wall, which is broken (arrowheads). Scale bar = 1 μm.

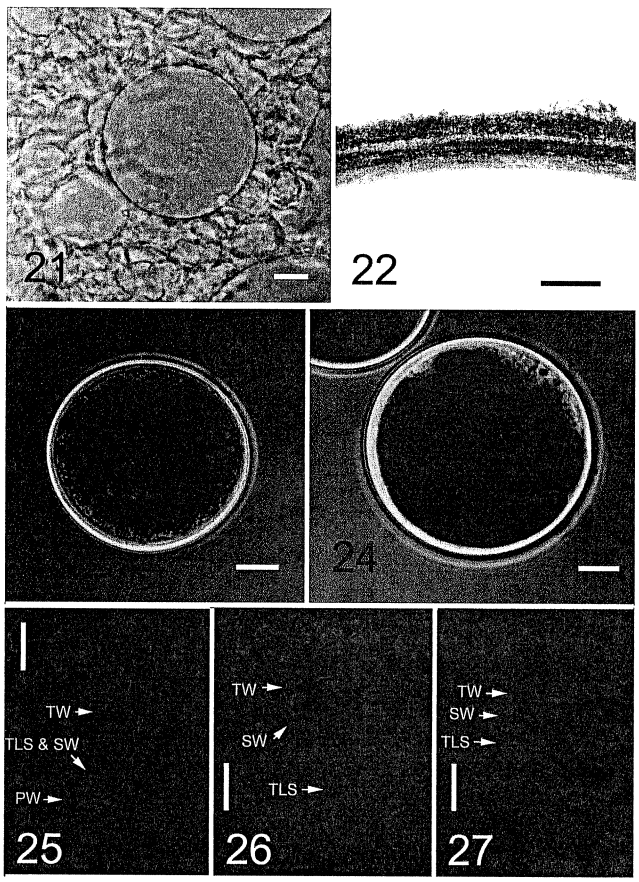

Figs 21–27. Cyst wall in *H. pluvialis.*

Figs 21, 22. Aceto-resistant wall material.

Fig. 21. Phase-contrast light microscopy. Note that the wall has conserved its spherical shape. Scale bar = 5 μm.

Fig. 22. TEM observation showing the undamaged trilaminar sheath. Scale bar = 0.2 μm.

Fig. 23. Intact cyst wall treated with 10% KOH. Scale bar = 5 μm.

Fig. 24. Intact cyst wall treated with 2-aminoethanol. Scale bar = 5 μm.

Figs 25–27. Fluorescence images of the cyst wall stained with Calcofluor White. Scale bar = 20 μm.

Fig. 25. Cyst wall without enzymatic treatments. Note the continuous fluorescence pattern.

Fig. 26. Cyst wall previously treated with cellulase. Note the decrease in fluorescence in the trilaminar sheath and the secondary wall, as well as the discontinuous fluorescence in the tertiary wall (arrows).

Fig. 27. Cyst treated with β-mannosidase. Fluorescence remained constant in the trilaminar sheath, it was slightly lower in the secondary wall, and it was discontinuous in the tertiary wall (arrows). PW, remnants of the primary wall; SW, secondary wall; TLS, trilaminar sheath; TW, tertiary wall.

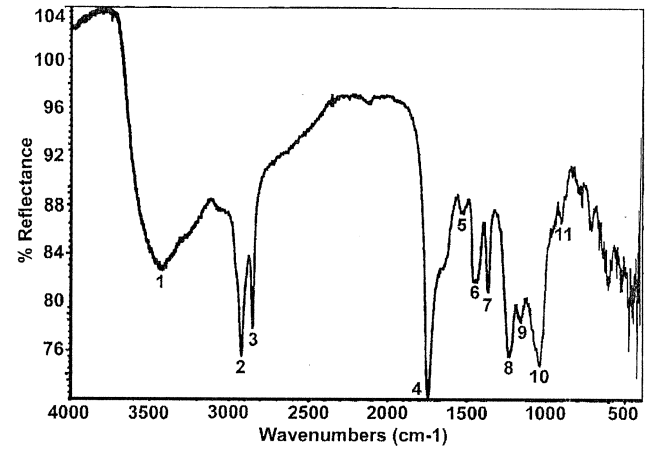

Fig. 28. Infrared absorption spectra of acetolysed residues from cysts of *H. pluvialis.* The numbers indicate the main group frequencies.

the cyst expansion all throughout the germination process. At the moment of zooid release, the tertiary wall broke only in the cyst's apical region, where it was much thinner. Although the secondary and tertiary walls appeared similar in mature cysts, the arrangement of their components during cyst formation was different. This may explain the different behaviour of these walls during germination. The released zoospores remained reddish as a result of the presence of astaxanthin in agreement with observations by Wang *et al.* (2003) at 72 h under 350 μmol photons m^{-2} s^{-1}.

The wall-breaking mechanism in *H. pluvialis,* which is followed by zooid release, could be compared to dehiscence and ascospore discharge in bitunicate asci of Ascomycetes, because as in our case the outer wall ruptures and the inner wall, or part of it, first elongates and then breaks to allow ascospore discharge through an apical pore (Eriksson 1981; Sherwood 1981). Similarly, although both ascus walls are composed of microfibrils embedded in an amorphous matrix, they differ from each other in the arrangement of microfibrils (Reynolds 1971).

Chemical characterization of the cyst wall

In the present research, the FT-IR absorbance profiles of the resulting material from cyst acetolysis of Argentinian *H. pluvialis* strains were similar to those of the aceto-resistant materials of Danish *H. pluvialis* strains according to the report by Montsant *et al.* (2001), except for the following differences: (1) the hydroxyl groups were relatively less important than either the aliphatic nature or the ester and ether contents; (2) absorption at 1740 cm^{-1} (C=O) was not complex and with a well-resolved strong band; and (3) the region between 1200 and 1000 cm^{-1} showed three signals instead of the two observed in the FT-IR absorbance profiles indicated by Montsant *et al.* (2001). In our material, a low level of unsaturation was

←

Fig. 18. Details of the basal portion of cyst where the tertiary wall has again adopted the same ultrastructural configuration as that observed during its synthesis (compare with Fig. 12). Scale bar = 0.5 μm.

Fig. 19. Details of an apical portion of a germinated cyst with a very thin, broken tertiary wall (arrowhead). Note that zooids conserve the astaxanthin content of the cyst. Scale bar = 5 m.

Fig. 20. Empty cyst (light micrograph). Scale bar = 5 μm. As, astaxanthin; N, nucleus; SW, secondary wall; TW, tertiary wall.

observed by the occurrence of weak absorptions around 1500 and 900 cm^{-1}, and a high aliphatic nature was confirmed by the presence of sharp peaks around 2900 cm^{-1}. Signal at *c.* 720 cm^{-1} indicated polymethylenic chains with $n > 4$. The aceto-resistant material also showed a high oxygen content caused by the formation of carboxylic acid esters in the hydroxyl groups due to partial acetylation during acetolysis ($-O-CO-CH_3$; i.e. bands at 1740, 1460, and 1370 cm^{-1}, respectively). Acetolysis enriched the isolated products from the cell walls in the hydrophobic layers (Rodríguez & Cerezo 1996). Polymethylenic chains were located primarily in the electron opaque bands of the trilaminar sheath and were cross-linked to fibrillar polysaccharides as cellulose (Rodríguez *et al.* 1999). The electron translucent band in the trilaminar sheath was composed primarily of polysaccharides. Still, these compounds were not fully eliminated after acetolysis, because algaenan provided a hydrophobic coating to the fibrils. In the infrared spectrum, bands corresponding to the fingerprint region of polysaccharides (1160–970 cm^{-1}) could be detected (i.e. 1140, 1050 cm^{-1}). In contrast, and in agreement with studies on algaenan (Rodríguez & Cerezo 1996; Rodríguez *et al.* 1999), our histochemical results showed no significant bands corresponding to phenolic compounds in the infrared spectrum. Negative staining with phloroglucinol was also indicative of the absence of lignin-like, acetolysis-resistant compounds in the cyst walls of *H. pluvialis.*

The strong aliphatic nature of the acetolysis-resistant product from *H. pluvialis* cysts highly resembles the spectra of algaenan isolated from other Chloroccocalean algae such as *Chlorella fusca* (Atkinson *et al.* 1972) rather than those of sporopollenin from pollen grains (Puel *et al.* 1987). The following phenomena also evidence the presence of an algaenan material in the resistant *H. pluvialis* cyst wall: its resistance to acetolysis, its degradation by exposure to chromic acid, and the fact that the cyst wall was unaffected by KOH and 2-aminoethanol. Insolubility in 2-aminoethanol was also observed in *Phycopeltis* walls (Good & Chapman 1978), *Chlamydomonas monoica* zygospores (VanWinkle-Swift & Rickoll 1997), and in other algae (Berkaloff *et al.* 1983). Bryophyte and pteridophyte spores also exhibited the same behaviour as that described above, while it was variable in different pollen grains (Southworth 1974). Sporopollenin from pollen grains has been reported to be altered by ethanolamine (Rowley & Flynn 1966; Sengupta & Rowley 1974; Southworth 1974; May *et al.* 1975).

The fluorescence loss detected in the trilaminar sheath in cysts of *H. pluvialis* treated with cellulase revealed the presence of cellulose in this sheath. The presence of cellulose was also observed in the trilaminar sheath fraction of *Coelastrum sphaericum,* which consisted mostly of algaenan and cellulose (Rodríguez *et al.* 1999). The fluorescence observations of *H. pluvialis* cysts also treated with mannosidase revealed the presence of mannose as well as of cellulose in their secondary and tertiary walls. The same composition has been observed in the fraction of the cell wall of the green alga *C. sphaericum* by means of methylation and spectroscopical analyses of DMSO-LiCL-solubilized fractions (Rodríguez *et al.* 1999). In cysts of German strains of *H. pluvialis,* gas chromatographic analyses of monosaccharides revealed mannose as the main part of wall carbohydrates (Hagen *et al.* 2002). In our study, fluorescence and TEM observations of *H. pluvialis* cysts clearly indicated that the cyst wall is composed of a fibrillar cellulose component immersed in an amorphous mannose fraction, the cellulose fibrils being homogeneously arranged in the secondary wall and heterogeneously displayed in the tertiary wall. Still, both extraction and a selective analysis of the components of these two walls are necessary to accurately assess their chemical structure and composition.

TEM observations of this aceto-resistant wall material confirmed its trilaminar aspect, which was identical to that of the trilaminar sheath of the zygospore wall of *C. monoica* (VanWinkle-Swift & Rickoll 1997). The presence of either a trilaminar structure in the outer wall is a common characteristic of these algaenan-producing organisms. Nonetheless, there are also exceptions to this common characteristic as evidenced by a few cases in which the presence of highly resistant wall material is not associated with the existence of a trilaminar structure, as in the cysts' wall of *Pyramimonas pseudoparkeae* (Aken & Pienaar 1985), in spores of *Spirogyra* (De Vries *et al.* 1983), and in mature zygotes of *Coleochaete* (Delwiche *et al.* 1989).

ACKNOWLEDGEMENTS

Financial support for the present research was provided by the Consejo Nacional de Investigaciones Científicas y Técnicas (CONICET), Argentina, through grants PEI 6024 and PIP 0949/98 to PIL and EJC, as well as by the Secretaría de Ciencia y Tecnología of the Universidad Nacional del Sur through grant PGI 488/03 to EJC. Thanks Dr C. Rodríguez for assistance with the fluorescence micrographs and for comments on the manuscript. We also thank Dr T. Motomura and reviewers for helpful suggestions to improve the manuscript. PIL is a researcher from the CONICET and EJC is a researcher from the Comisión de Investigaciones Científicas de la Provincia de Buenos Aires, Argentina.

REFERENCES

AKEN M.E. & PIENAAR R.N. 1985. Preliminary investigations on the chemical composition of the scale-boundary and cyst wall of *Pyramimonas pseudoparkeae* (Prasinophyceae). *South African Journal of Botany* 51: 408–416.

ATKINSON A.W. JR., GUNNING B.E.S. & JOHN P.C.L. 1972. Sporopollenin in the cell wall of *Chlorella* and other algae: ultrastructure, chemistry, and incorporation of ^{14}C-acetate, studied in synchronous cultures. *Planta* 107: 1–32.

BERKALOFF C., CASADEVALL E., LARGEAU C., METZGER P., PERACCA S. & VIRLET J. 1983. The resistant polymer of the walls of the hydrocarbon-rich alga *Botryococcus braunii. Phytochemistry* 22: 389–397.

BROWN D.L., LEPPARD G.G. & MASSALKI A. 1976. Fine structure of encystment of the Quadri Alga, *Polytomella agilis. Protoplasma* 90: 139–154.

BURCZYK J. 1987. Biogenetic relationships between ketocarotenoids and sporopollenins in green algae. *Phytochemistry* 26: 113–119.

DE VRIES P.J.R., SIMONS J. & VAN BEEM A.P. 1983. Sporopollenin in the spore wall of *Spirogyra* (Zygnemataceae, Chlorophyceae). *Acta Botanica Neerlandica* 32: 25–28.

DELWICHE C.F., GRAHAM L.E. & THOMSON N. 1989. Lignin-like compounds and sporopollenin in *Coleochaete,* an algal model for land plant ancestry. *Science* 245: 399–401.

ERIKSSON O. 1981. The families of bitunicate Ascomycetes. *Opera Botanica* 60: 1–220.

FAUST B. 1992. *Modern chemical techniques.* Royal Society of Chemistry, London.

FERRER N.C. & CÁCERES E.J. 1995. *Spirogyra salmonispora* sp.nov. (Zygnematophyceae, Chlorophyta), a new freshwater species of the section conjugata. *Archiv für Protistenkunde* 146: 101–106.

GOOD B.H. & CHAPMAN R.L. 1978. The ultrastructure of *Phycopeltis* (Chroolepidaceae: Chlorophyta). I. Sporopollenin in the cell walls. *American Journal of Botany* 65: 27–23.

HAGEN C., BRAUNE W. & BJÖRN L.O. 1994. Functional aspects of secondary carotenoids in *Haematococcus lacustris* [Girod] Rostafinski (Volvocales). III. Action as a "sunshade". *Journal of Phycology* 30: 241–248.

HAGEN C., GRÜNEWALD K., SCHMIDT S. & MÜLLER J. 2000. Accumulation of secondary carotenoids in flagellates of *Haematococcus pluvialis* (Chlorophyta) is accompanied by an increase in per unit chlorophyll productivity of photosynthesis. *European Journal of Phycology* 35: 75–82.

HAGEN C., GRÜNEWALD K., XYLÄNDER M. & ROTHE E. 2001. Effect of cultivation parameters on growth and pigment biosynthesis in flagellated cells of *Haematococcus pluvialis. Journal of Applied Phycology* 13: 79–87.

HAGEN C., SIEGMUND S. & BRAUNE W. 2002. Ultrastructural and chemical changes in the cell wall of *Haematococcus pluvialis* (Volvocales, Chlorophyta) during aplanospore formation. *European Journal of Phycology* 37: 217–226.

HARKER M., TSAVALOS A.J. & YOUNG A.J. 1996. Autotrophic growth and carotenoid protection of *Haematococcus pluvialis* in a 30 liter air-lift photobioreactor. *Journal of Fermentation and Bioengineering* 82: 113–118.

HOEN P. 2000. Glossary of Pollen and Spore Terminology. In Part 4 (P-R). http://www.biol.ruu.nl/~palaeo/glossary/glos-int.htm.

IVERSEN J. & TROELS-SMITH J. 1950. Pollenmorphologische definitonen und typen. *Danmarks Geologiske Undersogelse* Ser. 4. 3: 1–54.

JOHNSON E.A., VILLA T.G. & LEWIS M.J. 1980. *Phaffia rhodozyma* as an astaxanthin source in salmonid diets. *Aquaculture* 20: 123–134.

KOKOT S., TUAN N.A. & RINTOUL L. 1997. Discrimination of reactive dyes on cotton fabric by Raman Spectroscopy and Chemometrics. *Applied Spectroscopy* 51: 387–392.

MAY G., SOUTHWORTH D. & DICKINSON D. 1975. Analysis of sporopollenin isolated from pollen of *Ambrosia artemisiifolia* and *A. trifida. Grana* 15: 149–152.

MENDES-PINTO M.M., RAPOSO M.FJ., BOWEN J., YOUNG A.J. & MORAIS R. 2001. Evaluation of different cell disruption processes on encysted cells of *Haematococcus pluvialis*: effects on astaxanthin recovery and implications for bio-availability. *Journal of Applied Phycology* 13: 19–24.

MONTSANT A., ZARKA A. & BOUSSIBA S. 2001. Presence of a nonhydrolyzable biopolymer in the cell wall of vegetative cells and astaxanthin-rich cysts of *Haematocccus pluvialis* (Chlorophyceae). *Marine Biotechnology* 3: 515–521.

NAKANISHI K. & SOLOMON P.A. 1977. *Infrared absorption spectroscopy,* ed. 2. Holden-Day, San Francisco.

OSTERGAARD JENSEN M. & MOESTRUP O. 1997. Autecology of the toxic dinoflagellate *Alexandrium ostenfeldii*: life history and growth at different temperatures and salinities. *European Journal of Phycology* 32: 9–18.

PAPPAS C., RODIS P., TARANTILIS P.A. & POLOSSIOU M. 1999. Predictions of the pH in wood by diffuse reflectance infrared fourier-transform spectroscopy. *Applied Spectroscopy* 53: 805–810.

PRETSCH E., SEIBL J., SIMON W. & CLERC T. 1983. *Tables of spectral data for structure determination of organic compounds.* Springer-Verlag, Heidelberg, Germany.

PUEL F., LARGEAU C. & GIRAUD G. 1987. Occurrence of a resistant biopolymer in the outer walls of the parasitic alga *Prototheca wickerhamii* (Chlorococcales): ultrastructural and chemical studies. *Journal of Phycology* 23: 649–656.

REYMOND O.L. & PICKETT-HEAPS J.D. 1983. A routine flat embedding method for electron microscopy of microorganisms allowing selection and precisely orientated sectioning of single cells by light microscopy. *Journal of Microscopy* 130: 79–84.

REYNOLDS D.R. 1971. Wall structure of a bitunicate ascus. *Planta* 98: 244–257.

RODRÍGUEZ M.C. & CEREZO A.S. 1996. The resistant "biopolimer" in cell walls of *Coelastrum sphaericum. Phytochemistry* 43: 731–734.

RODRÍGUEZ M.C., NOCEDAL M.D. & CEREZO A.S. 1999. The fibrillar polysaccharides and their linkage to algaenan in the trilaminar layer of the cell wall of *Coelastrum sphaericum* (Chlorophyceae). *Journal of Phycology* 35: 1025–1031.

ROWLEY J.R. & FLYNN J.J. 1966. Single-stage carbon replicas of microspores. *Stain Technology* 41: 287–290.

SENE C.F.B., MCCANN M.C., WILSON R.H. & GRINTER R. 1994. Fourier-transform raman and Fourier-transform infrared spectroscopy (an investigation of five higher plant cell walls and their components). *Plant Physiology* 106: 1623–1631.

SENGUPTA S. & ROWLEY J.R. 1974. Re-exposure of tapes at high temperatures and pressure in *Lycopodium clavatum* spore exine. *Grana* 14: 143–151.

SHERWOOD M.A. 1981. Convergent evolution in Discomycetes from bark and wood. *J. Linnean Society of London Botany* 82: 15–34.

SOUTHWORTH D. 1974. Solubility of pollen exines. *American Journal of Botany* 61: 36–44.

STEIN J.R. 1973. *Handbook of phycological methods. Culture methods and growth measurements.* Cambridge University Press, Cambridge, U.K. 448 pp.

VANWINKLE-SWIFT K.P. & RICKOLL W.L. 1997. The zygospore wall of *Chlamydomonas monoica* (Chlorophyceae): morphogenesis and evidence for the presence of sporopollenin. *Journal of Phycology* 33: 655–665.

WANG B., ZARKA A., TREBST A. & BOUSSIBA S. 2003. Astaxanthin accumulation in *Haematococcus pluvialis* (Chlorophyceae) as an active photoprotective process under high irradiance. *Journal of Phycology* 39: 1116–1124.

Received 2 May 2005; accepted 30 March 2006
Associate editor: T. Motomura